Dana L Wright, David G. Kimmel, Nancy Robertson, and David Strausz
Title: Joint species distribution modeling reveals a changing prey landscape for North Pacific right whales on the Bering shelf
Journal: Ecological Applications

Section S1. Species data

Table S1. List of species included in analysis.

Species	Stages/sizes included in modeling
Acartia spp.	mixed
Amphipoda	< 5 mm
Calanus glacialis	C2, C3, C4, C5, C6 (Adult)
Chaetognatha	<5 mm, 5-20 mm, > 20 mm
Cnidaria	< 5 mm, > 5 mm
Decapoda	Juvenile + Adult
Eucalanus bungii	C5, C6 (Adult)
Euphausiid	nauplius, calyptosis
Limacina helicina	< 5 mm
Metridia spp.	C1, C2, C3, C4, C5, C6 (Adult)
Mysidae	mixed
Neocalanus cristatus	C5
Neocalanus spp.	C1-C4
Oithiona spp.	C5 + Adult
Ostracoda	< 5 mm
Pseudocalanus spp.	C1, C2, C3, C4, C5, C6 (Adult)
Thysanoessa inermis	Juvenile + Adult
Thysanoessa longipes	Juvenile + Adult
Thysanoessa raschii	Juvenile + Adult
Thysanoessa spinifera	Juvenile + Adult

Section S2. Model Description

The model gjamTime is a discrete-time dynamic biophysical food web model that links an extended LV model (Equation 1) to gjam (generalized joint attribute modeling; Clark et al. 2017). Briefly, gjam is fitted with a Bayesian hierarchical multivariate tobit-regression model that uses data censoring to allow inclusion of multifarious response data (e.g., discrete abundance, continuous, categorical, etc.) as well as a high degree of zeros that are commonly found in ecological data into one model. The gjam model provides probabilistic uncertainty of parameters, model specification, and data. Also, the model can quantify the likelihood of species

to covary on the scale of individual species, which is useful for rare or poorly sampled species. The gjam model also avoids non-linear link functions, which provides more intuitive and transparent responses for ecological interpretation. The gjam framework has been successfully applied to terrestrial (e.g., O'Reilly-Nugent et al., 2018; Bossolani et al., 2021) and marine systems (e.g., Howe-Kerr et al., 2019; Roberts et al., 2022). A wonderful comparison of model fitting groundfish species abundance data from the Northwest Atlantic using gjam versus the generalized additive model (GAM) framework is found in Roberts et al. (2022).

The DD matrix $\boldsymbol{\alpha}_s$ in gjamtime is a prior for the model. By allowing for species interactions in $\boldsymbol{\alpha}_s$ across the discrete time-steps, nonlinear response patterns between species and environment can be observed even though all relationships between species and environment are modeled as linear in gjamTime, because nonlinear response patterns are induced indirectly from the differential response of other species to the same gradient over the discrete time-series. Put another way, gjamTime does not hard-code nonlinear responses to environment (e.g., x_i^2, where i is a given environmental term); instead, gjamTime allows each species in the community to respond linearly to environment (x_i) and experience species interactions over the discrete time-steps ($\boldsymbol{\alpha}_s$), which should induce nonlinear curves to x_i for species where density dependence influences dynamics in the given environment (e.g., common prey, common predator, etc.; Hutchinson 1957).

References

Bossolani, J.W., Crusciol, C.A.C., Leite, M.F.A., Merloti, LF., Moretti, L.G., Pascoaloto, I.M., and Kuramae, E.E. 2021. "Modulation of the soil microbiome by long-term Ca-based soil

amendments boosts soil organic carbon and physiochemical quality in a tropical no-till crop rotation system." *Soil Biology and Biochemistry* 156: 108188.

Clark, J.S., Nemergut, D., Seyednasrollah, B., Turner, P., and Zhang. S. 2017. "Generalized joint attribute modeling for biodiversity analysis: Median-zero, multivariate, multifarious data." *Ecological Monographs* 87: 34–56.

Howe-Kerr, L.I., Bachelot, B., Wright, R.M., Kenkel, C.D., Bay, L.K., Correa, A.M.S. 2019. "Symbiont community diversity is more variable in corals that respond poorly to stress." *Global Change Biology* 26: 2220–2234.

Hutchinson, G. E. 1957. Concluding remarks – Cold Spring Harbor Symposium, Quantitative Biology, 22: 415-427.

O'Reilly-Nugent, A., Wandrag, E.M., Catford, J.A., Gruber, B., Driscoll, D., and Duncan, R.P. 2018. "Measuring competitive impact: Joint-species modeling of invaded plant communities." *Journal of Ecology* 108: 449–459.

Roberts, S.M., Halpin, P.N. and Clark, J.S. 2022. Jointly modeling marine species to inform the effects of environmental change on an ecological community in the Northwest Atlantic. *Scientific Reports 12*(1): 132.

Section S3. Modeling terms

Section S3.1 Potential density-independent (DI) growth terms

In situ bottom (BT) and surface Temperature (ST) data were collected from the National Marine Fisheries Service (NMFS) eastern Bering Sea shelf standardized bottom trawl survey, which has been conducting annual summer (May-August) surveys within a systematic grid design since 1982 (Lauth et al., 2019). Water temperatures were recorded at each station by a Sea-Bird SBE-

39 datalogger (Sea-Bird Electronics, Inc., Bellevue, WA) placed on the headrope of the net. Surface temperature was recorded at -1 m depth, and bottom temperature was averaged over time while the net was on bottom in fishing configuration, with the headrope 2-3 m off bottom. Data were averaged per grid square for each year using the *Spatial Join* tool in ArcGIS Pro. Data are available at https://www.fisheries.noaa.gov/inport/item/22008#lineage.

Section S3.2. Potential 'movement' terms (immigration/emigration)

The Bering Sea cold pool has traditionally been derived from the NMFS bottom trawl survey data by interpolating the aerial extent (km^2) of the cold pool (defined as <2 °C) by inverse-distance-weighting (IDW) bottom temperatures on the Being Shelf using geostatistical software (Kotwicki & Lauth, 2013, Stevenson & Lauth, 2019). To maximize spatial and temporal resolution in our model, we computed the percent aerial cold pool extent for each grid square for each year, defined as pCP. We also used pCP instead of aerial cold pool extent because the aerial cold pool was highly correlated with aerial sea ice extent (Pearson product correlation >0.8 at α = 0.5; data not shown).

To calculate pCP, we first interpolated the cold pool across the Bering Shelf (0 – 300 m) for an area buffered 50km from the bottom trawl sampling grid using the *EKB Regression Prediction* tool in ArcGIS Pro (hereafter EKB RP). EKB RP combines kriging with regression analysis to make predictions. We chose EKB RP to allow bathymetry to impact the cold pool structure. We ran EKB RP models on untransformed data with the environmental predictor bathymetry (General Bathymetric Chart of the Oceans 2019 dataset; https://www.gebco.net/) for four semivariograms (nugget, exponential, Whittle, and K-Bessel) for one *cold* year (2012) and one *warm* year (2015); we then compared models using leave one out cross validation to

determine the best model. All models were run for 100 simulated variograms with 100 points in each local model, a local model overlap factor of 1, and a smooth circular search neighborhood (smoothing factor 0.2). K-Bessel semivariograms performed best for both years (Appendix S1: Table S3). Therefore, the cold pool was interpolated for each year to be used in modeling (2005-2016) using K-Bessel semivariogram models. We then converted the model output to an integer raster using the *Raster Calculator* tool and isolated areas on the map for each year with bottom temperatures ≤ 2 °C using *Con* tool. Finally, we calculated the percent areal extent per grid square by first summing the Con output using *Zonal Statistics as Table* and then calculating the aerial percentage using the *Calculate Field* tool. We note that the interpolation of the NOAA grid did not cover the full range of the northern grid square; nevertheless, we assumed 100% cold pool coverage in that grid square for each year, because sea-ice seasonally covered this area and formed a cold pool in this region across our study period (Stabeno & Bell, 2019; Huntington et al., 2020).

Two wind metrics – wind direction and wind gusts - were derived from the ERA5 hourly data on single levels from 1979 to present dataset (0.25° grid cells for every third hour (e.g., 0000, 0300, 0600, etc.) between 55–63°N and -176 to -160°W from 2004 to 2017; https://cds.climate.copernicus.eu/cdsapp#!/dataset/reanalysis-era5-single-levels?tab=overview; obtained 1 September 2021). Wind direction data were defined as southeasterly (SE) and northwesterly (NW) winds for winter (Oct-Apr; SEw, NWw) and summer (May-Sep; SEs, NWs) based off prior modeling in the region (Danielson et al., 2012; Eisner et al., 2014). These data were derived from uwind and vwind data 10 m above the ocean surface. The hourly uwind and vwind data were imported as netcdfs, masked to the study region, and converted to directional degree before mean direction values were calculated per grid square at each timestep. From this,

the percentage of days with seasonal wind from each direction was computed for each grid by year and season. Analysis was completed using R packages *raster* (v 3.3-7; Hijams, 2020), *sf* (v 0.9-4; Pebesma, 2018), and *dplyr*, and visualized with *ggplot2* (v 3.3.5; Wickham, 2016).

For wind gusts, we calculated seasonal wind gusts – summer [WGs] and winter [WGw] – as well as shorter-term transitional periods – Apr-May [WGsp] and Sep-Oct [WGf] – from instantaneous wind gusts (m/s) measured 10 m above the ocean surface. Pearson production correlations were used to define the shorter-term transitional periods that were not highly correlated with the seasonal wind gust terms (Appendix S1: Figure S1). We used the workflow above for wind direction except that we calculated the number of days with wind above a given threshold for each grid instead of a percentage. We used wind gust thresholds of >10 m/s and >15 m/s based on prior work in the region (Bond et al., 1994; Stabeno et al., 2010); these thresholds also provided the largest range in values over the study domain (Appendix S1: Figure S2).

Annual oceanographic variables and indices were downloaded from the NOAA Bering Climate website (http://www.beringclimate.noaa.gov/data/index.php; accessed 10 October 2021). Variables include: Aleutian Low (Nov-Mar; AL), Arctic Oscillation (Dec-Feb; AO), East Pacific Index for winter (Jan-Mar; EPIw) and spring-summer (Apr-Jul; EPIss), North Pacific Index for winter (Nov-Mar; NPIw) with anomaly (NPIAw) and spring-summer (Apr-Jul; NPIss) with anomaly NPIAss), and Pacific Decadal Oscillation for winter (Dec-Feb; PDOw), summer (June-Aug; PDOs), and annual (Jan-Dec; PDO).

Days with ice after 15 March (IDm) were derived for each 80km grid cell from the *"Bootstrap Sea Ice Concentrations from Nimbus-7 SMMR and DMSP SSM/I-SSMIS, Version 3"* dataset from the National Snow and Ice Data Center (*nsidc.org*). This data has a 25km

resolution. An 80 km^2 box was created around each desired data point and ice data from the dataset was averaged from inside the box. Ice associated days were defined as having greater than 15% ice coverage inside the box.

To incorporate space into the model, latitude (Lat) was determined for each grid square using the *Feature to Point* and *Add XY Coordinates* Tools in ArcGIS Pro.

References

ArcGIS Pro. 2020. Version 2.5. Redlands, CA: Environmental Systems Research Institute, Inc., 2010. https://www.esri.com/en-us/arcgis/products/arcgis-pro/

Bond, N.A., Overland, J.E., and Turet, P. 1994. "Spatial and temporal characteristics of the windn forcing in the Bering Sea." *American Meteorological Society* 7: 1119–1130.

Danielson, S., Hedstrom, K., Aagaard, K., Weingartner, T., and Curchitser, E. 2012. "Wind-induced reorganization of the Bering shelf circulation." *Geophysical Research Letters* 39: L08601.

Eisner, L.B., Napp, J.M., Mier, K.L., Pinchuk, A.I., and Andrews, A.J. III. 2014. "Climate-mediated changes in zooplankton community structure for the eastern Bering Sea." *Deep-Sea Research II* 109: 157–171.

Hijams, R.J. 2020. "raster: geographic data Analysis and Modeling." R package version 3.3-7. https://CRAN.R-project.org/package=raster.

Huntington, H.P., Danielson, S.L., Wiese, F.K., Baker, M., Boveng, P., Citta, J.J., De Robertis, A., Dickson, D.M.S., Farley, E., George, J.G., Iken, K., Kimmel, D.G., Kuletz, K., Ladd, C., Levine, R., Quakenbush, L., Stabeno, P., Stafford, K.M., Stockwell, D., and Wilson,

C. 2018. “Evidence suggests potential transformation of the Pacific Arctic ecosystem is underway.” *Nature Climate Change* 10: 342-348.

Kotwicki, S., & Lauth, R.R. 2013. “Detecting temporal trends and environmentally-driven changes in the spatial distribution of bottom fishes and crabs on the eastern Bering Sea shelf.” *Oceanography* 94: 231-243.

Lauth, R., Dawson, R., E. J., and Conner, J. 2019. “Results of the 2017 eastern and northern Bering Sea continental shelf bottom trawl survey of groundfish and invertebrate fauna.” U.S. Department of Commerce, NOAA Tech Memo. NMFS-AFSC-396, 260 p.

Pebesma, E. 2018. “Simple Features for R: Standardized Support for Spatial Vector Data.” *The R journal* 10(1): 439-446. https://doi.org/10.32614/RJ-2018-009.

Stabeno, P., Napp, J., Mordy, C., and Whitledge, T. 2010. Factors influencing physical structure and lower trophic levels of the eastern Bering Sea shelf in 205: Sea ice, tides, and winds.” *Progress in Oceanography* 85: 180-196.

Stabeno, P., and Bell, S.W. 2019. “Extreme conditions in the Bering Sea (2017-2018): Record-breaking low sea-ice extent.” *Geophysical Research Letters* 46: 8952–8959.

Stevenson, D.E., and Lauth, R.R. 2018. “Bottom trawl surveys in the northern Bering Sea indicate recent shifts in the distribution of marine species.” *Polar Biology* 42: 407-421.

Wickham, H. 2016. “ggplot2: Elegant Graphics for Data Analysis.” *Springer-Verlag New York*.

Wickham, H., François, R., Henry, Lionel, and Müller, K. 2020. “dplyr: A Grammar of Data Manipulation.” R package version 1.0.0. https://CRAN.R-project.org/package=dplyr.

Table S2. Potential environmental variables for model fitting of movement (beta) and DI growth (rho) terms in model, ordered alphabetically; bold indicates variables used in model fitting following removal of redundant variables via Pearson production correlation with preference given to variables that vary in space and time (Appendix S1: Figure S1). Note that DI growth and movement terms are computed independently in the model.

Label	Variable	Model	Resolution of data	Resolution in model	Data source
AL	**Aleutian Low (Nov-Mar)**	**Beta**	**CI**	**CI**	**BCW[#]**
AO	Arctic Oscillation (Dec-Feb)	Beta	CI	CI	BCW[#]
BT	**Bottom Temperature (°C)**	**Rho**	**Tow**	**80 km GS**	**AFSC***
CP	Cold Pool Extent (km^2)	Beta	BS	BS	BCW[#]
EPIss	East Pacific Index – spring/summer (Apr-Jul)	Beta	CI	CI	BCW[#]
EPIw	East Pacific Index – winter (Jan-Mar)	Beta	CI	CI	BCW[#]
IDm	**Days with Ice > 15 March (# days)**	**Beta**	**25 km cell**	**80 km GS**	**NSIDC[%]**
IE	**Ice extent (km^2)**	**Beta**	**BS**	**BS**	**BCW[#]**
Lat	**Latitude**	**Beta**	**GC**	**80 km GS**	**ArcGIS Pro**
NPIAss	N. Pacific Index anomaly – spr/summer (Apr-Jul)	Beta	CI	CI	BCW[#]
NPIAw	N. Pacific Index anomaly - winter (Nov-Mar)	Beta	CI	CI	BCW[#]
NPIss	N. Pacific Index – summer (Apr-Jul)	Beta	CI	CI	BCW[#]
NPIw	N. Pacific Index - winter (Nov-Mar)	Beta	CI	CI	BCW[#]
NWs	**Northwesterly winds - summer (May-Sep) (%)**	**Beta**	**0.25°cell**	**80 km GS**	**ERA5[^]**
NWw	**Northwesterly winds - winter (Oct-Apr) (%)**	**Beta**	**0.25°cell**	**80 km GS**	**ERA5[^]**
pCP	**Percentage of cold pool per grid square (%)**	**Beta**	**BS**	**80 km GS**	**Derived BT**
PDOa	Pacific Decadal Oscillation - annual (Jan-Dec)	Beta	CI	CI	BCW[#]
PDOs	Pacific Decadal Oscillation - summer (Jun-Aug)	Beta	CI	CI	BCW[#]
PDOw	Pacific Decadal Oscillation - winter (Dec-Feb)	Beta	CI	CI	BCW[#]
SEs	**Southeasterly winds - summer (May-Sep) (%)**	**Beta**	**0.25°cell**	**80 km GS**	**ERA5[^]**
SEw	**Southeasterly winds - winter (Oct-Apr) (%)**	**Beta**	**0.25°cell**	**80 km GS**	**ERA5[^]**
ST	**Surface Temperature (°C)**	**Rho**	**CTD cast**	**80 km GS**	**AFSC***
WGf	**Wind gusts - fall (Sep-Oct) (# days)**	**Beta**	**0.25°cell**	**80 km GS**	**ERA5[^]**
WGs	**Wind gusts - summer (May-Sep) (# days)**	**Beta**	**0.25°cell**	**80 km GS**	**ERA5[^]**
WGsp	**Wind gusts - spring (Apr-May) (# days)**	**Beta**	**0.25°cell**	**80 km GS**	**ERA5[^]**
WGw	**Wind gusts - winter (Oct-Apr) (# days)**	**Beta**	**0.25°cell**	**80 km GS**	**ERA5[^]**

CI = Climatological index; GC = Geographic coordinate; BS = Bering shelf; 80 km GS = 80-kilometer grid square; *AFSC = NOAA Alaska Fisheries Science Center; [%]NSIDC = National Snow and Ice Data Center (https://nsidc.org/); [^]ERA5 hourly data fifth generation ECMWF Uwind, Vwind, and wind gusts (European Center for Medium-Range Weather Forecasts, https://cds.climate.copernicus.eu/cdsapp#!/home); [#]Bering Climate Website, https://www.beringclimate.noaa.gov/. Wind gusts were computed with threshold of 10 and 15 m/s.

Table S3. Leave-one-out cross validation results for EKB Regression Prediction cold pool interpolation models from 2012 and 2015. SE = Standard Error; RMSE = Root Mean Square Error. Bold denotes the best model for each year.

		Model	Mean Prediction Error	Standardized Mean Prediction Error	Avg SE	RMSE	Avg SE - RMSE	Avg RMSE
2012	Stratified	Exponential	-0.052	-0.0332	0.5895	0.5376	0.0519	0.8226
		K-Bessel	-0.055	-0.0441	0.5730	0.5344	0.0386	0.8538
		Nugget	-0.066	0.0294	1.3714	1.1956	0.1758	0.8434
		Whittle	-0.054	-0.0399	0.5602	0.5304	0.0298	0.8646
	Non-stratified	Exponential	-0.007	-0.0014	0.5102	0.4799	0.0303	0.9182
		K-Bessel	**-0.008**	**-0.0008**	**0.4650**	**0.4733**	**-0.0083**	**0.9818**
		Nugget	-0.293	-0.1720	1.3680	1.0882	0.2798	0.7813
		Whittle	-0.007	-0.0013	0.5103	0.4799	0.0304	0.9182
2015	Stratified	Exponential	-0.001	-0.0090	0.5371	0.4626	0.0745	0.8995
		K-Bessel	-0.010	-0.0110	0.4966	0.4573	0.0393	0.9484
		Nugget	-0.211	-0.1590	1.5824	1.0512	0.5312	0.7138
		Whittle	-0.009	-0.0075	0.5046	0.45807	0.0465	0.9346
	Non-stratified	Exponential	-0.003	-0.0040	0.4888	0.4543	0.0345	0.9604
		K-Bessel	**-0.005**	**-0.0079**	**0.4555**	**0.4546**	**0.0009**	**1.0008**
		Nugget	-0.057	-0.0490	1.5463	1.1729	0.3734	0.7717
		Whittle	-0.004	-0.0075	0.4604	0.4528	0.0076	0.9994

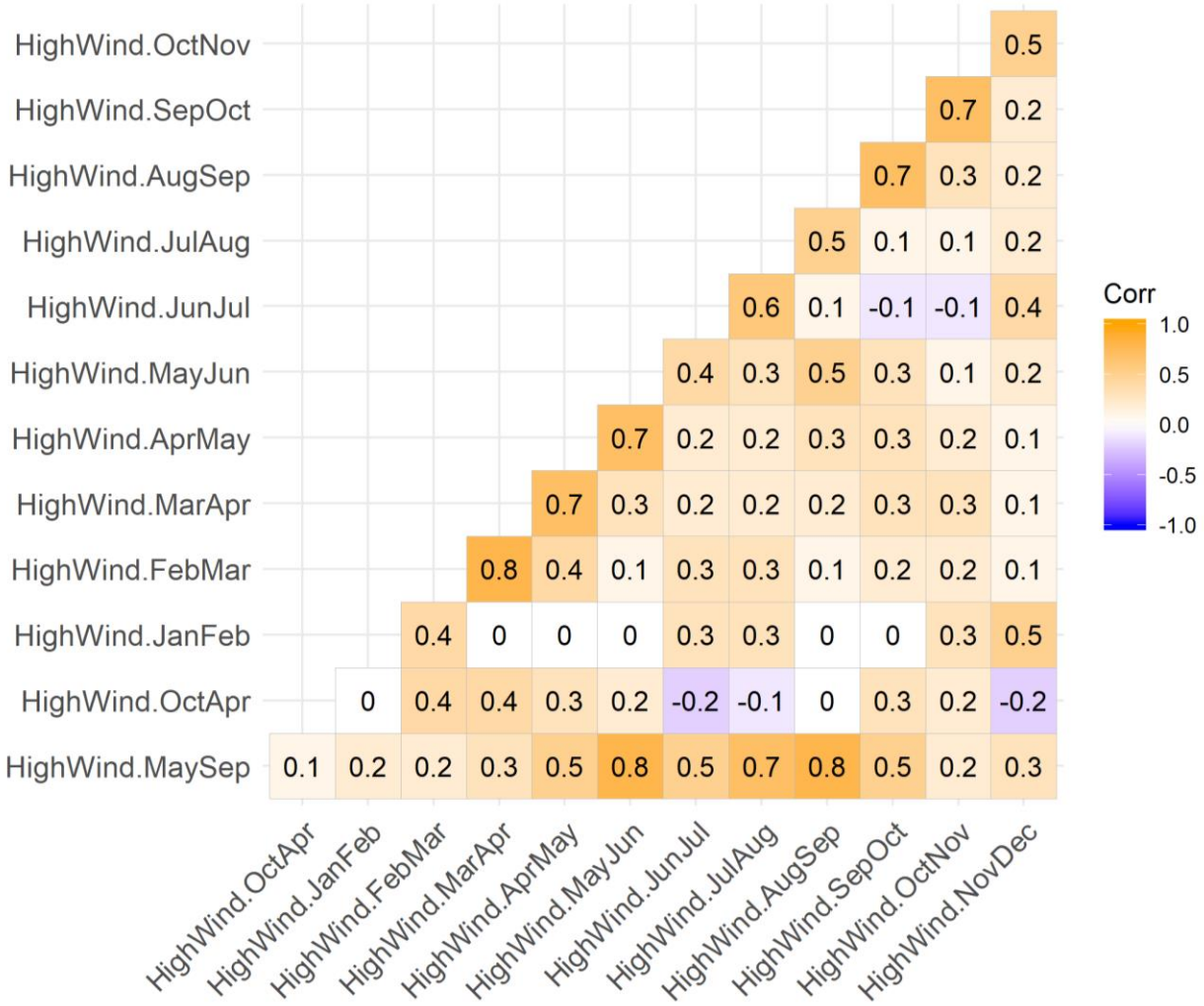

Figure S1. Pearson product correlation matrix of wind gusts >10 m/s in two-month increments. Out of the spring and fall months with variable wind gusts across the study domain (Appendix S1: Figure S2), only Apr-May and Sep-Oct were correlated <0.7 with 'summer' winds (May-Sep); the correlation threshold of 0.7 was used when deciding which variables to include in model fitting (Dormann et al. 2013). Consequently, the 'spring' transition was defined as Apr-May and the fall transition was defined as Sep-Oct.

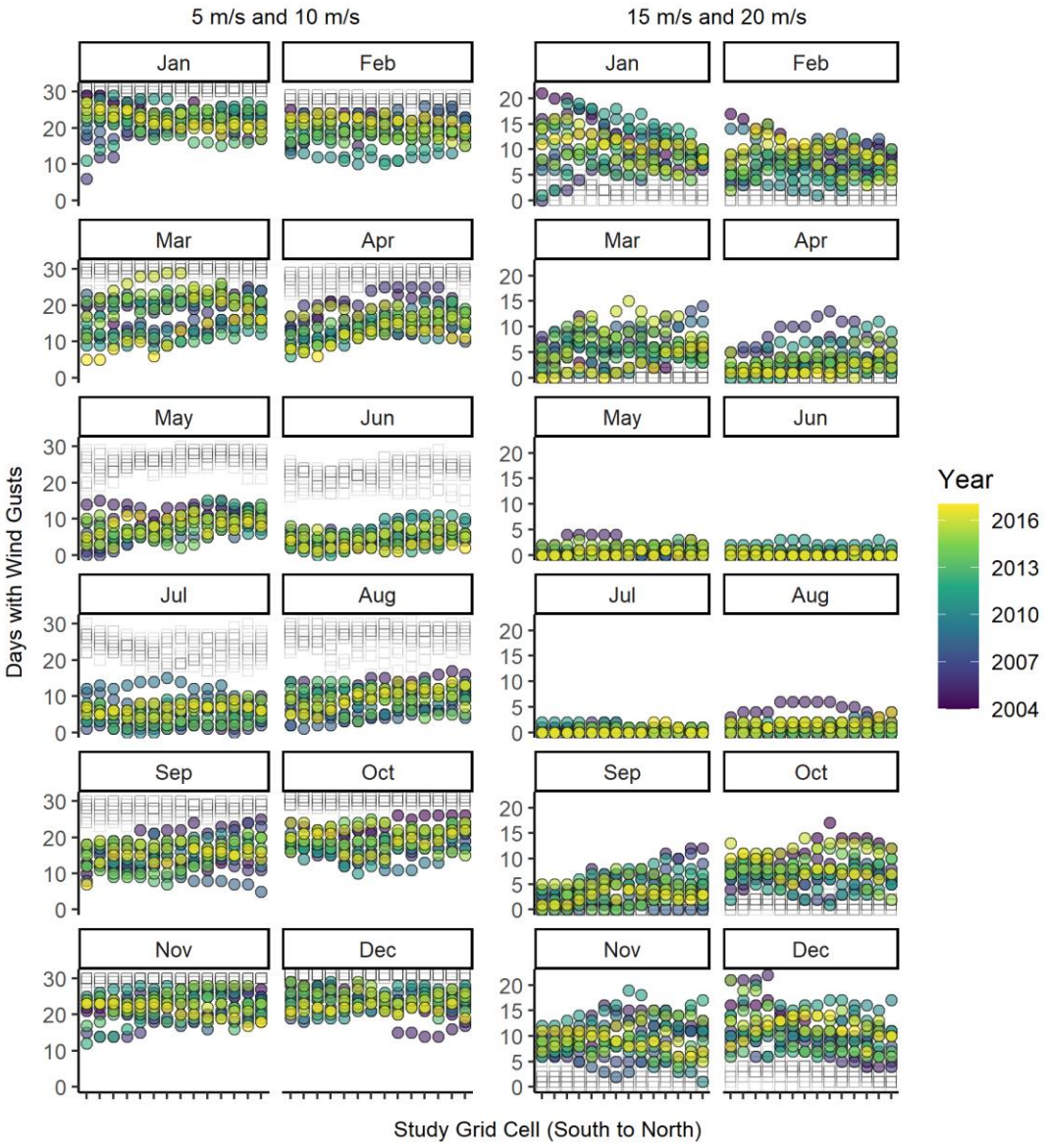

Figure S2. Number of days above wind gust threshold by month for each 80 km grid cell (arranged south to north) from 2004-2016. Left panel denotes wind gust thresholds of 5 m/s (gray boxes) and 10 m/s (colored circles); right panel denotes wind gust thresholds of 15 m/s (colored circles) and 20 m/s (gray boxes). Data derived from every third hour of ERA5 hourly instantaneous wind gusts at 10 m above the ocean surface (https://cds.climate.copernicus.eu/cdsapp#!/home).

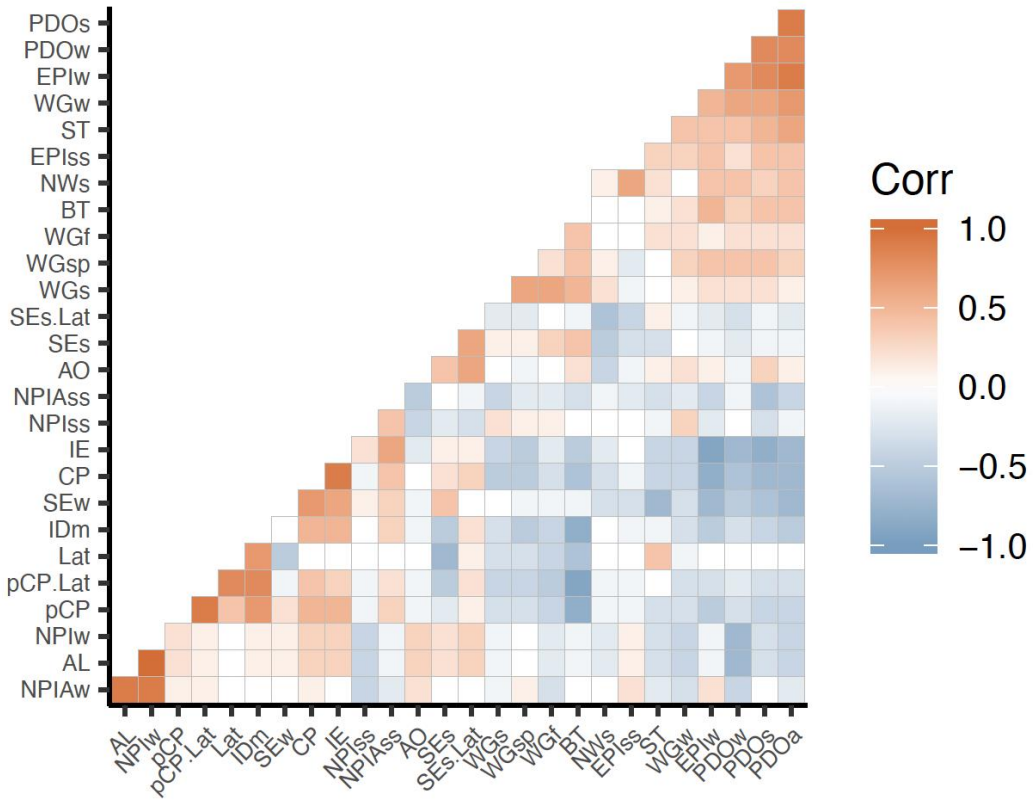

Figure S3. Pearson product correlation matrix of potential environmental variables for model fitting. Wind gusts were computed with threshold of 10 and 15 m/s; figure shows threshold of 15 m/s. The subset of variables selected for modeling are listed in Table 1. Note that DI growth and movement terms are computed independently in the model; therefore, redundancy in potential environmental DI growth variables is independent of potential movement variables; consequently, high correlations between DI growth and movement terms were ignored when determining variable redundancy.

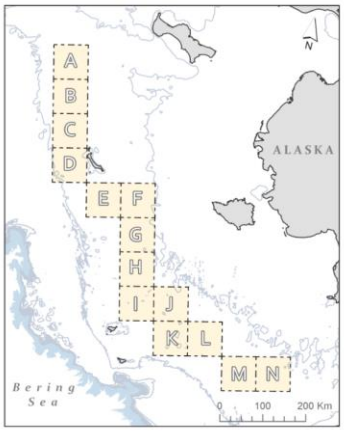

	A	B	C	D	E	F	G	H	I	J	K	L	M	N
2006	+	+	+	+	+	+	+	+	+	+	+	+	+	+
2007	+	+	+	+	+	+	+	+	+	+	+	+	+	+
2008	+	+	+	+	+	+	+	+	+	+	+	+	+	+
2009	+	+	+	+	+	+	+	+	+	+	+	+	+	+
2010	+	+	+	+	+	+	+	+	+	+	+	+	+	+
2011					+				+	+	+	+	+	+
2012	+	+	+	+	+	+	+	+	+	+	+	+	+	+
2013														
2014	+	+	+	+	+	+	+	+	+	+	+	+	+	+
2015	+	+	+	+	+	+	+	+	+	+	+	+	+	+
2016					+	+	+	+	+	+	+	+	+	+

Figure S4. Grid cells with zooplankton data (+) by year and cell. Bathymetric contour lines presented in 50 m increments from 50 to 2,000 m depth (blue gradient from dark to light).

Section S4. Model Prior and Effort

The current version of gjamTime requires *informative* priors. DI growth ($\boldsymbol{\rho}$) priors are in units of change in DI growth per time-step (here annual). We defined priors -1 to 1 to allow 100% change in DI growth between time-steps given the *in-situ* patchiness and varying life history strategy of zooplankton species included in our study. Movement **($\boldsymbol{\beta}$)** priors are in units of the response divided by the predictor. We therefore defined movement priors -0.5 to 0.5 for pCP and -1 to 1 for all other variables. Effort was defined as 1 for all time-steps with data and 0.1 for priors and missing data to be imputed (smaller effort priors translate to lower weighting of data; Clark et al. 2020).

References

Clark, J.S., Scher, C.L. and Swift, M. 2020. "The emergent interactions that govern biodiversity change." *Proceedings of the National Academy of Sciences* 117(29): 17074–17083.

Section S5. Model diagnostics

Model fit was assessed using the diagnostic plots provided in the R *gjam* package (Clark et al., 2017), namely observed vs. prediction plots and inverse prediction. The best model was defined as the model that could best predict the abundance of *C. glacialis* (Appendix S1: Figure S5). This best model best predicted life history stages of *C. glacialis* followed by *T. raschii* and *T. inermis* (Appendix S1: Figure S6). Predictions of other species in the assemblage were variable, but in general, species sampled consistently and with higher abundance were better predicted. Inverse predictions (*i.e.*, using the zooplankton responses from the fitted model to model the environmental predictors) provide a powerful metric to assess model fit, because they inform whether the observed responses are dependent on the predictors at the community scale (Clark et al., 2017). The best model of potential right whale prey inverse predicted bottom temperature and spring and fall winds but failed to inverse predict surface temperature (Appendix S1: Figure S7).

References

Clark, J.S., Nemergut, D., Seyednasrollah, B., Turner, P., and Zhang. S. 2017. "Generalized joint attribute modeling for biodiversity analysis: Median-zero, multivariate, multifarious data." *Ecological Monographs* 87: 34–56.

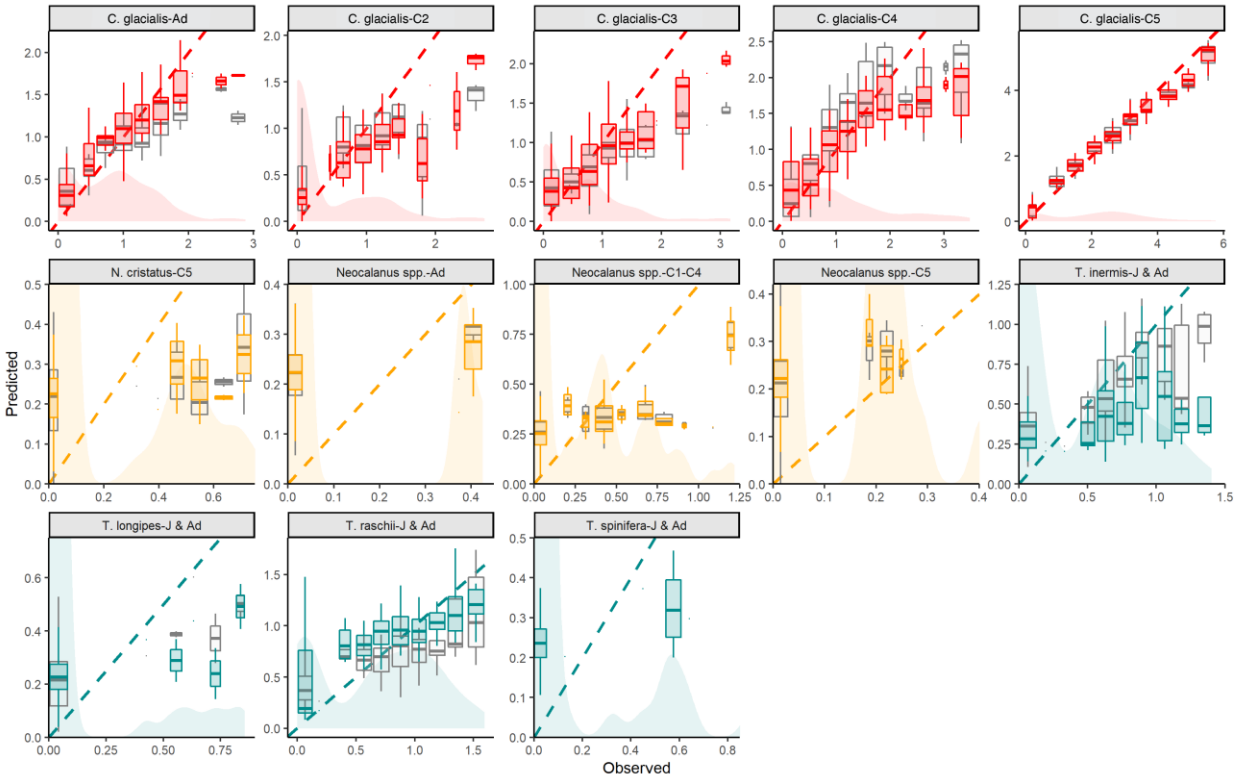

Figure S5. Predicted and observed observations from the 'best' fitted model, defined as the best fit of *C. glacialis* copepodite stages (colored boxes) and lowest DIC model (gray boxes) for *C. glacialis*, *Neocalanus* spp., and *Thysanoessa* spp. Boxes and whiskers bound 68% and 95% of observations, respectively. Background shading denotes the distribution of data.

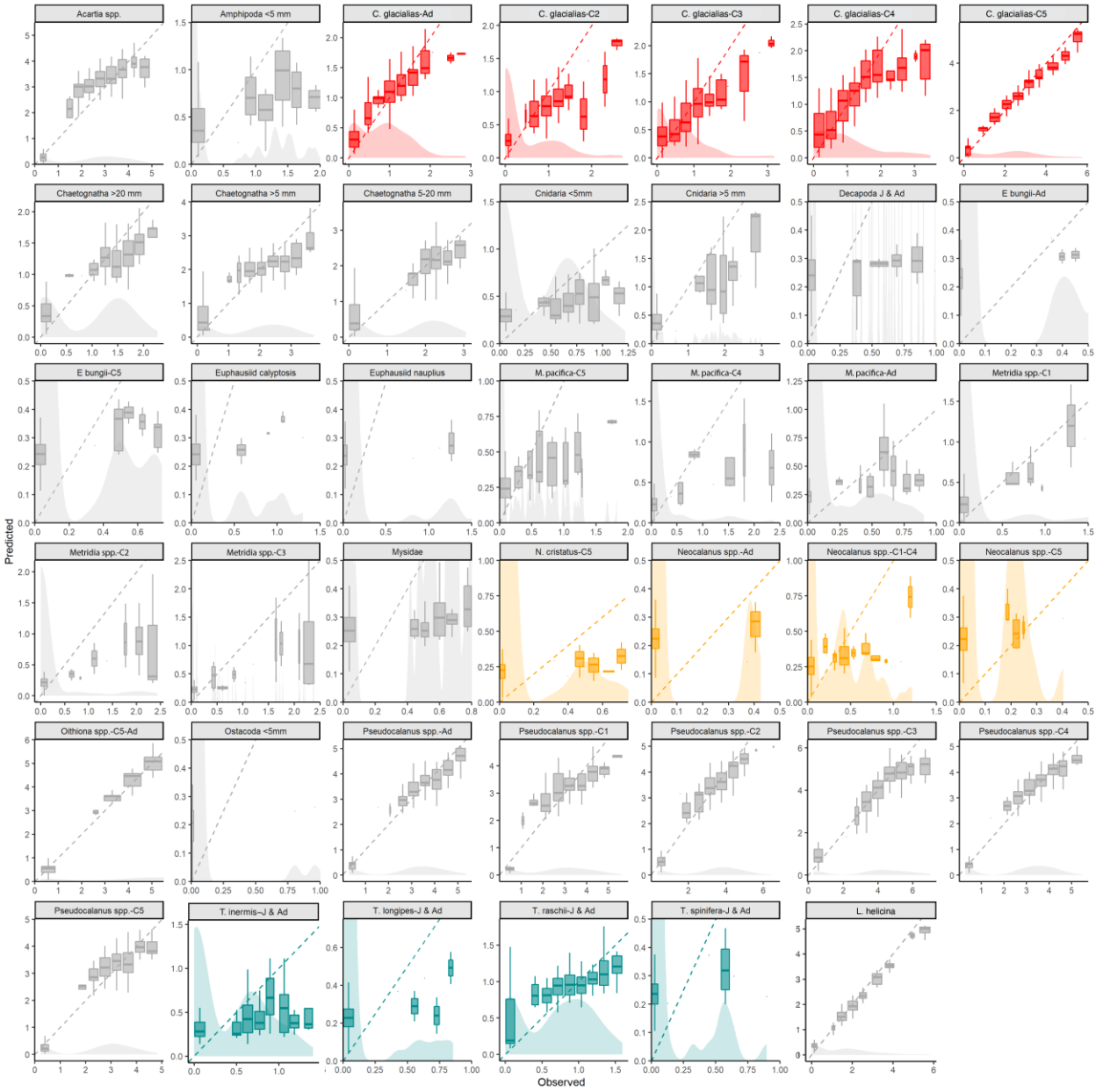

Figure S6. Predicted and observed observations of all zooplankton species from the best fitted model. Boxes represent medians with 25th through 75th percentiles and whiskers bound ±1.5*IQR (Inner Quartile Range) of the posterior distribution, respectively. Colors correspond to potential right whale prey species (red = *C. glacialis*; orange = *Neocalanus* species, and teal = *Thysanoessa* species). Background shading denotes the distribution of data.

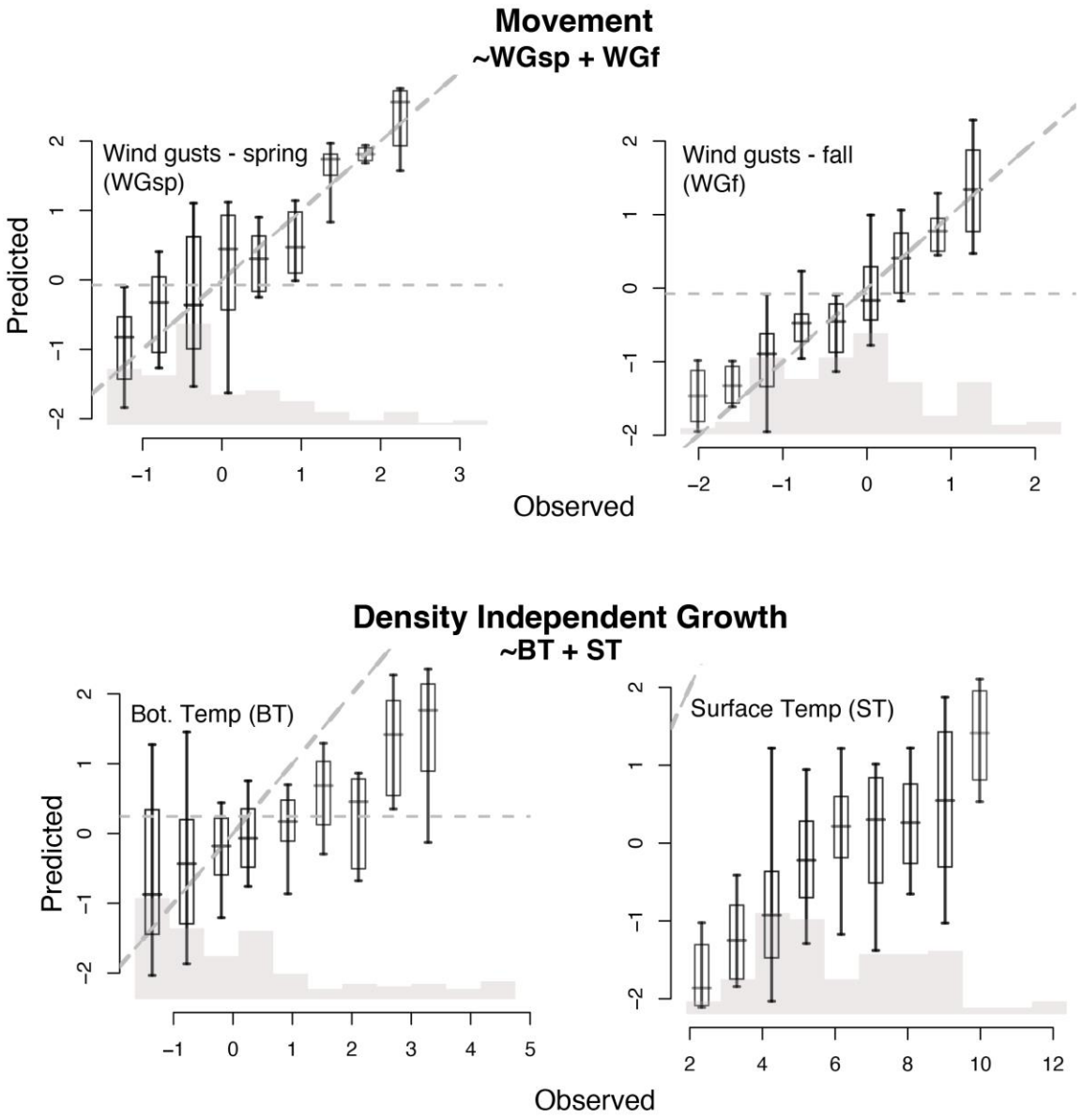

Figure S7. Inverse prediction of environmental variables for (upper) the fitted movement model (spring and fall wind gusts) and (lower) the density-independent growth model (bottom and surface temperature). Boxes and whiskers bound 68% and 95% of the posterior distribution, respectively. Basal histogram shows the distribution of the data.

Section S6. Model results

Table S4. Modeled parameter estimates, standard error, and 95% Bayesian credible intervals of beta term (movement) bottom temperature to species abundance (ind. m^{-3}). Sig. = significance of response defined as 95% credible interval away from zero.

Species	Estimate	SE	2.5% CI	97.5% CI	Sig.
Acartia spp.	0.04	0.02	0.00	0.08	*
Amphipoda < 5 mm	0.00	0.06	-0.12	0.11	
C. glacialis - C2	-0.11	0.10	-0.31	0.08	
C. glacialis - C3	-0.07	0.04	-0.16	0.01	*
C. glacialis - C4	-0.09	0.03	-0.16	-0.03	*
C. glacialis - C5	-0.01	0.02	-0.05	0.03	
C. glacialis - Adult	-0.04	0.04	-0.12	0.03	
Chaetognatha < 5 mm	0.05	0.02	0.02	0.09	*
Chaetognatha – 5 – 20 mm	-0.10	0.03	-0.17	-0.04	*
Chaetognatha > 20 mm	-0.11	0.05	-0.21	-0.02	*
Cnidaria < 5 mm	-0.07	0.03	-0.13	-0.01	*
Cnidaria > 5 mm	0.08	0.06	-0.04	0.20	
Decapoda J & Ad	-0.01	0.12	-0.26	0.23	
E. bungii - C5	0.00	0.17	-0.33	0.33	
E. bungii - Adult	0.33	0.38	-0.49	0.95	
Euphausiid Nauplius	-0.02	0.06	-0.15	0.10	
Euphausiid Calyptosis	-0.02	0.07	-0.15	0.11	
Limacina helicina < 5 mm	-0.04	0.02	-0.08	0.00	
Metridia spp. - C1	-0.40	0.11	-0.61	-0.17	*
Metridia spp. - C2	-0.25	0.05	-0.34	-0.16	*
Metridia spp. - C3	-0.18	0.04	-0.26	-0.10	*
Metridia pacifica - C4	-0.15	0.06	-0.27	-0.03	*
Metridia pacifica - C5	0.07	0.06	-0.05	0.19	
Metridia pacifica - Adult	-0.38	0.10	-0.57	-0.18	*
Mysidae	0.10	0.10	-0.10	0.29	
N. cristatus - C5	0.22	0.37	-0.53	0.90	
Neocalanus spp. C1-C4	0.38	0.36	-0.36	0.96	
Neocalanus spp. - C5	0.06	0.20	-0.32	0.44	
Neocalanus spp. - Adult	0.00	0.51	-0.91	0.91	
Oithiona spp. C5 & Ad	0.06	0.01	0.04	0.08	*
Ostracoda < 5 mm	-0.23	0.26	-0.74	0.29	
Pseudocalanus spp. - C1	0.11	0.02	0.07	0.15	*
Pseudocalanus spp. - C2	0.07	0.02	0.04	0.10	*
Pseudocalanus spp. - C3	0.03	0.01	0.01	0.06	*
Pseudocalanus spp. - C4	0.03	0.02	0.00	0.06	

Pseudocalanus spp. - C5	0.03	0.02	0.00	0.07	
Pseudocalanus spp. - Adult	0.00	0.01	-0.03	0.03	
Thysanoessa inermis - J & Ad	0.07	0.04	-0.02	0.15	
Thysanoessa longipes - J & Ad	0.02	0.17	-0.30	0.36	
Thysanoessa raschii - J & Ad	0.09	0.04	0.01	0.17	*
Thysanoessa spinifera - J & Ad	0.17	0.16	-0.15	0.50	

Table S5. Modeled parameter estimates, standard error, and 95% Bayesian credible intervals of beta term (movement) surface temperature to species abundance (ind. m^{-3}). Sig. = significance of response defined as 95% credible interval away from zero.

Species	Estimate	SE	2.5% CI	97.5% CI	Sig.
Acartia spp.	0.03	0.01	0.00	0.05	
Amphipoda < 5 mm	-0.01	0.02	-0.05	0.02	
C. glacialis - C2	-0.01	0.02	-0.04	0.02	
C. glacialis - C3	0.04	0.02	0.01	0.07	
C. glacialis - C4	0.02	0.01	0.00	0.04	
C. glacialis - C5	-0.05	0.01	-0.07	-0.03	*
C. glacialis - Adult	-0.07	0.01	-0.08	-0.05	*
Chaetognatha < 5 mm	-0.02	0.01	-0.05	0.00	*
Chaetognatha – 5 – 20 mm	-0.08	0.01	-0.09	-0.06	
Chaetognatha > 20 mm	-0.09	0.01	-0.11	-0.06	*
Cnidaria < 5 mm	0.06	0.01	0.04	0.08	
Cnidaria > 5 mm	0.03	0.02	-0.02	0.08	
Decapoda J & Ad	-0.03	0.03	-0.09	0.03	
E. bungii - C5	0.01	0.04	-0.08	0.09	
E. bungii - Adult	-0.02	0.11	-0.24	0.19	
Euphausiid Nauplius	0.00	0.04	-0.09	0.07	
Euphausiid Calyptosis	0.00	0.03	-0.06	0.05	
Limacina helicina < 5 mm	0.10	0.01	0.09	0.11	*
Metridia spp. - C1	0.06	0.02	0.01	0.10	*
Metridia spp. - C2	0.07	0.02	0.03	0.10	*
Metridia spp. - C3	0.06	0.02	0.02	0.10	*
Metridia pacifica - C4	0.00	0.02	-0.05	0.05	
Metridia pacifica - C5	0.05	0.02	0.00	0.09	*
Metridia pacifica - Adult	0.23	0.05	0.13	0.32	*
Mysidae	0.00	0.03	-0.06	0.06	*
N. cristatus - C5	0.00	0.05	-0.11	0.11	
Neocalanus spp. C1-C4	0.03	0.09	-0.15	0.18	
Neocalanus spp. - C5	0.00	0.03	-0.07	0.06	
Neocalanus spp. - Adult	-0.21	0.09	-0.38	-0.02	
Oithiona spp. C5 & Ad	0.01	0.01	-0.01	0.02	
Ostracoda < 5 mm	-0.06	0.05	-0.16	0.03	
Pseudocalanus spp. - C1	0.01	0.01	-0.01	0.02	
Pseudocalanus spp. - C2	0.00	0.01	-0.02	0.02	
Pseudocalanus spp. - C3	0.01	0.01	0.00	0.02	
Pseudocalanus spp. - C4	0.02	0.01	0.00	0.04	
Pseudocalanus spp. - C5	0.02	0.01	0.00	0.04	

Pseudocalanus spp. - Adult	0.00	0.00	-0.01	0.01
Thysanoessa inermis - J & Ad	0.02	0.02	-0.02	0.06
Thysanoessa longipes - J & Ad	0.04	0.04	-0.04	0.12
Thysanoessa raschii - J & Ad	0.03	0.02	-0.01	0.06
Thysanoessa spinifera - J & Ad	0.00	0.05	-0.10	0.10

Table S6. Modeled parameter estimates, standard error, and 95% Bayesian credible intervals of rho term (DI growth) spring wind gusts (WGsp) to species abundance (ind. m^{-3}). Sig. = significance of response defined as 95% credible interval away from zero.

Species	Estimate	SE	2.5% CI	97.5% CI	Sig.
Acartia spp.	-0.01	0.16	-0.34	0.28	
Amphipoda < 5 mm	-0.17	0.07	-0.31	-0.03	*
C. glacialis - C2	-0.10	0.11	-0.31	0.11	
C. glacialis - C3	-0.16	0.07	-0.30	-0.02	*
C. glacialis - C4	-0.40	0.08	-0.57	-0.24	*
C. glacialis - C5	-0.40	0.15	-0.70	-0.13	*
C. glacialis - Adult	-0.22	0.09	-0.39	-0.06	*
Chaetognatha < 5 mm	0.14	0.15	-0.16	0.42	
Chaetognatha – 5 – 20 mm	0.01	0.15	-0.30	0.29	
Chaetognatha > 20 mm	-0.01	0.09	-0.19	0.16	
Cnidaria < 5 mm	0.23	0.07	0.09	0.36	*
Cnidaria > 5 mm	0.10	0.05	0.00	0.19	*
Decapoda J & Ad	-0.06	0.05	-0.16	0.03	
E. bungii - C5	-0.01	0.05	-0.10	0.09	
E. bungii - Adult	0.03	0.05	-0.07	0.12	
Euphausiid Nauplius	-0.02	0.05	-0.12	0.07	
Euphausiid Calyptosis	0.00	0.05	-0.09	0.10	
Limacina helicina < 5 mm	-0.44	0.16	-0.77	-0.13	*
Metridia spp. - C1	0.11	0.10	-0.07	0.34	
Metridia spp. - C2	-0.03	0.07	-0.17	0.12	
Metridia spp. - C3	0.08	0.06	-0.05	0.20	
Metridia pacifica - C4	-0.12	0.05	-0.22	-0.02	*
Metridia pacifica - C5	-0.12	0.06	-0.23	-0.01	*
Metridia pacifica - Adult	0.03	0.05	-0.07	0.12	
Mysidae	0.02	0.05	-0.08	0.11	
N. cristatus - C5	-0.10	0.06	-0.22	0.02	
Neocalanus spp. C1-C4	-0.04	0.05	-0.14	0.07	
Neocalanus spp. - C5	-0.01	0.05	-0.11	0.09	
Neocalanus spp. - Adult	0.00	0.05	-0.11	0.10	
Oithiona spp. C5 & Ad	0.21	0.31	-0.46	0.76	
Ostracoda < 5 mm	0.12	0.06	0.00	0.25	
Pseudocalanus spp. - C1	0.32	0.16	-0.02	0.60	
Pseudocalanus spp. - C2	0.38	0.21	-0.07	0.76	
Pseudocalanus spp. - C3	0.59	0.21	0.14	0.96	*
Pseudocalanus spp. - C4	0.28	0.16	-0.06	0.56	
Pseudocalanus spp. - C5	0.07	0.16	-0.26	0.35	

Pseudocalanus spp. - Adult	0.24	0.16	-0.09	0.52	
Thysanoessa inermis - J & Ad	0.11	0.05	0.01	0.21	*
Thysanoessa longipes - J & Ad	0.04	0.05	-0.06	0.14	
Thysanoessa raschii - J & Ad	-0.08	0.08	-0.25	0.08	
Thysanoessa spinifera - J & Ad	0.05	0.05	-0.04	0.15	

Table S7. Modeled parameter estimates, standard error, and 95% Bayesian credible intervals of rho term (DI growth) fall wind gusts (WGf) to species abundance (ind. m^{-3}). Sig. = significance of response defined as 95% credible interval away from zero.

Species	Estimate	SE	2.5% CI	97.5% CI	Sig.
Acartia spp.	-0.07	0.17	-0.43	0.24	
Amphipoda < 5 mm	0.06	0.07	-0.09	0.20	
C. glacialis - C2	-0.10	0.08	-0.25	0.05	
C. glacialis - C3	-0.17	0.07	-0.31	-0.03	*
C. glacialis - C4	-0.24	0.08	-0.41	-0.08	*
C. glacialis - C5	-0.10	0.14	-0.37	0.19	
C. glacialis - Adult	-0.09	0.08	-0.26	0.07	
Chaetognatha < 5 mm	-0.40	0.15	-0.68	-0.11	*
Chaetognatha – 5 – 20 mm	-0.34	0.14	-0.61	-0.05	*
Chaetognatha > 20 mm	-0.22	0.09	-0.39	-0.05	*
Cnidaria < 5 mm	-0.11	0.07	-0.25	0.03	
Cnidaria > 5 mm	0.00	0.06	-0.11	0.12	
Decapoda J & Ad	0.06	0.05	-0.04	0.17	
E. bungii - C5	-0.05	0.05	-0.15	0.05	
E. bungii - Adult	-0.04	0.05	-0.14	0.06	
Euphausiid Nauplius	0.00	0.05	-0.10	0.10	
Euphausiid Calyptosis	0.00	0.05	-0.10	0.10	
Limacina helicina < 5 mm	0.22	0.17	-0.12	0.55	
Metridia spp. - C1	-0.08	0.07	-0.22	0.05	
Metridia spp. - C2	-0.06	0.07	-0.19	0.07	
Metridia spp. - C3	-0.09	0.07	-0.22	0.04	
Metridia pacifica - C4	-0.02	0.05	-0.12	0.09	
Metridia pacifica - C5	-0.03	0.06	-0.14	0.08	
Metridia pacifica - Adult	-0.06	0.05	-0.16	0.05	
Mysidae	-0.01	0.05	-0.12	0.10	
N. cristatus - C5	-0.04	0.05	-0.15	0.06	
Neocalanus spp. C1-C4	0.00	0.05	-0.10	0.10	
Neocalanus spp. - C5	-0.09	0.05	-0.20	0.02	
Neocalanus spp. - Adult	-0.01	0.05	-0.11	0.09	
Oithiona spp. C5 & Ad	-0.17	0.31	-0.80	0.43	
Ostracoda < 5 mm	-0.05	0.06	-0.17	0.06	
Pseudocalanus spp. - C1	0.11	0.16	-0.24	0.41	
Pseudocalanus spp. - C2	-0.05	0.21	-0.51	0.34	
Pseudocalanus spp. - C3	-0.11	0.22	-0.57	0.29	
Pseudocalanus spp. - C4	-0.06	0.17	-0.42	0.24	
Pseudocalanus spp. - C5	-0.13	0.17	-0.48	0.18	

Pseudocalanus spp. - Adult	0.01	0.17	-0.34	0.32
Thysanoessa inermis - J & Ad	-0.02	0.05	-0.13	0.09
Thysanoessa longipes - J & Ad	-0.05	0.05	-0.16	0.05
Thysanoessa raschii - J & Ad	-0.13	0.09	-0.30	0.05
Thysanoessa spinifera - J & Ad	-0.01	0.05	-0.12	0.09

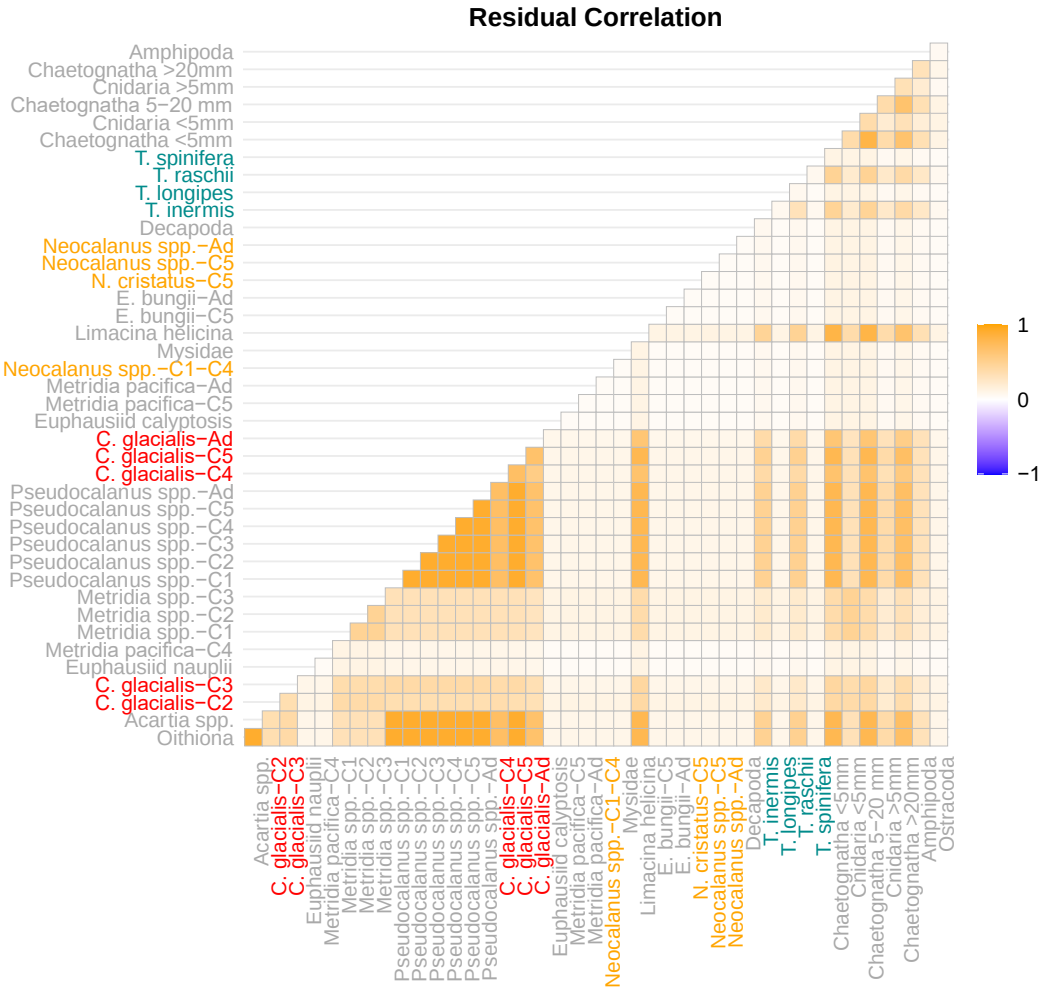

Figure S8. Residual correlation plot. Species are ordered by guild (microzooplankton predator, small omnivore, small-med omnivore, large omnivore, predators, and epibenthic); colors denote genus (red = *C. glacialis*, orange = *Neocalanus* species, teal = *Thysanoessa* species, and gray = other species). High correlation observed between small guilds, chaeotognath predators, *Thecosomata*, *T. inermis*, and *T. raschii*.

Section S7. Equilibrium abundance trends

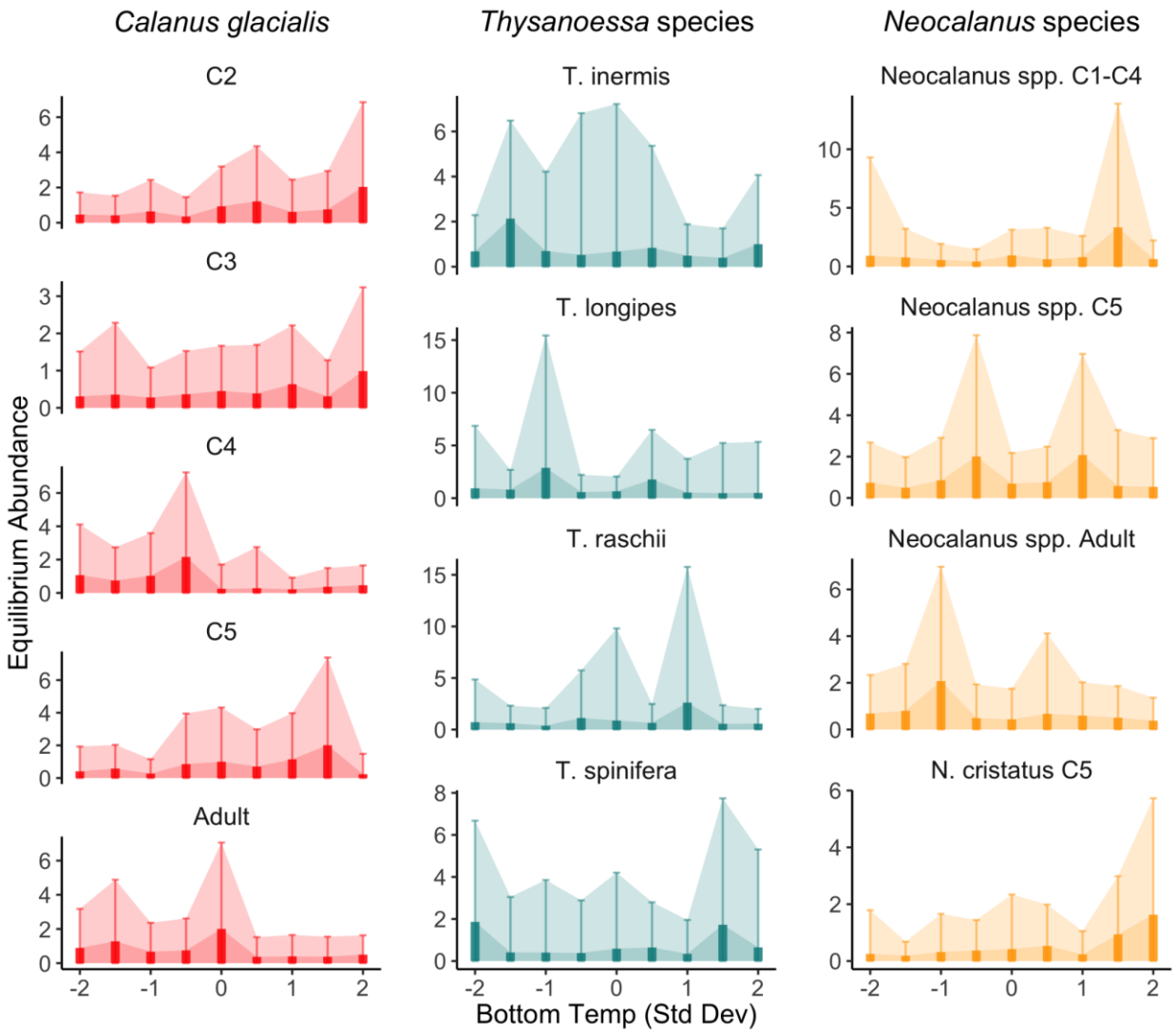

Figure S9. Predicted equilibrium abundance of *Calanus glacialis* (red), *Thysanoessa* species (teal), and *Neocalanus* species (orange) along a bottom water gradient for the model output with movement terms, spring and fall wind gusts, and DI growth (rho) terms, bottom and surface temperature. Thick bars bound 68% and thin bars bound 95% predictive intervals. Note that abundance is on the model output scale (fourth root transformed).